ISIJ International, Vol. 54 (2014), No. 12, pp. 2860–2867

Sliding Wear Behavior of PVD CrN and TiN Coated Austempered Ductile Iron

Diego Alejandro COLOMBO,[1,2)]* María Dolores ECHEVERRÍA,[1,2)] Sebastián LAINO,[2)] Ricardo Cesar DOMMARCO[2)] and Juan Miguel MASSONE[2)]

1) Mechanical Technology Group, School of Engineering–Universidad Nacional de Mar del Plata, Av. J. B. Justo 4302, B7608FDQ Mar del Plata, Argentina. 2) Metallurgy Division, INTEMA–CONICET, School of Engineering–Universidad Nacional de Mar del Plata, Av. J. B. Justo 4302, B7608FDQ Mar del Plata, Argentina.

(*Received on April 4, 2014; accepted on July 28, 2014*)

This work studies the sliding wear behavior of PVD coated austempered ductile iron samples. The effects of the substrate surface finishing method (grinding and polishing) and coating material (CrN and TiN) on the wear behavior are evaluated. Coatings were applied in an industrial reactor. Deposition times were adjusted to obtain similar film thicknesses in both coating materials. Wear tests under dry sliding conditions were carried out with a pin–on–disc tribometer (ASTM G99). The steady–state friction coefficient and wear rate were calculated for each sample variant. The wear track of the discs was examined by using optical microscopy and stylus profilometry.

The results obtained indicate that the uncoated and TiN coated samples show steady–state friction coefficients close to 0.8, while the CrN coated samples show steady–state values close to 0.4. The sliding wear tests do not produce the fracture and/or delamination of the films in any case. The specific wear rate of the CrN and TiN coated samples is close to zero, while that of the uncoated samples is higher. The wear rate of the uncoated samples is slightly higher for the ground ones. The specific wear rate of the pins (AISI 52100 bearing balls) is higher than that of the discs in all the cases. The wear rate of the pins tested against uncoated samples is higher for the ground ones. The wear rate of the pins tested against coated samples is higher for the polished and TiN coated ones.

KEY WORDS: austempered ductile iron; surface finishing; physical vapor deposition; TiN; CrN; sliding wear.

1. Introduction

Austempered ductile iron (ADI) is increasingly being used for the manufacturing of mechanical components given the wide range of mechanical properties achievable after the proper adjustment of the chemical composition and heat treatment parameters, as well as its advantageous features if compared to high–strength cast steels, such as its lower cost and weight, greater flexibility in parts design and comparable tensile strength.[1–3)] This material is widely used in mechanical applications characterized by dry as well as lubricated sliding conditions. Typical examples are disc brakes, piston rings, cylinder liners, railroad shoes, conveyors for abrasive ores and pump bearings.

Several authors have studied the sliding wear behavior of ADI.[4–7)] They found that austempering improves the wear resistance of ductile and gray iron. In addition, ADI wear resistance increases as austempering temperature decreases. The superior wear resistance of ADI with respect to ductile and gray iron may be attributed to the higher hardness brought about by the ausferrite structure and the work hardening of the surface as retained austenite is transformed to martensite by plastic deformation.[6–8)]

Material loss in ADI occurs mainly by delamination, which is related to the formation and growth of sub–surface cracks at local regions (nodule interfaces) of severe plastic deformation.[9–11)] Consequently, the use of surface treatments could offset the negative effect of the surface and sub–surface nodules. Different methods such as surface melting, surface hardening and surface alloying have been used to improve the sliding wear resistance of ADI.[12–15)] These methods modify the ADI microstructure by forming a hard layer on the surface. A modified case hardening technique called boro–tempering, which combines boronizing with austempering, has also been used.[16)] Boro–tempering heat treatment increases the wear resistance of ductile iron.

During the last decade, significant advances have been made in the application of PVD coatings of different materials on ADI substrates. Several authors have accounted for improvements in high cycle fatigue resistance, corrosion resistance and hardness.[17–20)] More recent studies have reported that electroless nickel (EN) and PVD–CrTiAlN duplex coatings provide better performance against erosive wear than monolithic EN or CrTiAlN coatings do. Moreover, the duplex coatings achieve a remarkable reduction in ADI's friction coefficient.[21)] The modern PVD techniques have allowed to use processing temperatures as low as

* Corresponding author: E-mail: diegocolombo@fi.mdp.edu.ar
DOI: http://dx.doi.org/10.2355/isijinternational.54.2860

230°C and thus to apply coatings on ductile iron parts previously austempered above this temperature without altering their microstructure.

Moreover, the authors of the present work found a combination of industrial–use processing parameters producing PVD TiN and CrN coatings of acceptable characteristics as far as film thickness, hardness, residual stresses and adhesion are concerned, causing no significant deterioration of ADI microstructure. Additionally, the analysis of the effects of the substrate characteristics on coating properties evidenced little influence of the austempering temperature and nodule count.[22–24] More recently, the rolling contact fatigue (RCF) behavior of PVD CrN and TiN coated ADI samples was studied.[25] It was found that the RCF resistance of coated samples is lower than that of uncoated samples. Failures in coated samples are mainly characterized by coating delamination and, to a lesser extent, by spall formation in the substrate. Graphite nodules present on the substrate surface act as preferential sites for coating fracture and subsequent delamination.

Grinding is one of the most commonly used processes in the industry when it comes to surface finishing of mechanical components. The abrasive cutting of grinding produces some degree of plastic deformation and high temperatures in the workpiece–wheel contact area, depending on the workpiece material, wheel characteristics and grinding variables such as workpiece speed, wheel speed and depth of cut per pass. As a result, surface hardening and residual stresses are generated, which may affect the service behavior of the components whether coated or not.

The authors of the present work studied the effect of grinding on the RCF behavior of PVD CrN and TiN coated ADI samples.[25] It was found that the substrates surface hardening caused by the plastic deformation associated to the abrasive cutting of grinding improves the RCF resistance of the uncoated and coated samples.

On this basis and in order to produce further advances, this work studies the dry sliding wear behavior of PVD coated ADI samples. The effects of the substrate surface finishing method (grinding and polishing) and coating material (CrN and TiN) on the friction coefficient and wear rate are evaluated.

2. Experimental Procedures

2.1. Substrate Material and Samples Preparation

The ductile iron utilized in this work was produced in a 55 kg middle–frequency induction furnace (3 kHz). The melt was conventionally nodulized and inoculated[22] and then poured into horizontal sand molds designed to obtain 70 mm diameter and 10 mm thick discs. The chemical composition of the material (wt%), analyzed by optical emission spectrometry, was as follows: C=3.35; Si=2.87; Mn=0.13; S=0.015; P=0.032; Mg=0.043; Cu=0.76; Ni=0.57 and Fe balanced. The carbon equivalent was eutectic (CE=4.32). Based on chart comparisons (ASTM A247), nodularity exceeded 90% in all cases. The discs were cut and machined by turning, in order to obtain the test samples illustrated in **Fig. 1**.

Afterwards samples were subjected to an austempering heat treatment, consisting in austenitising at 910°C for 120 min, austempering in a salt bath at 280°C for 90 min, and subsequently air cooling to room temperature. According to the aforementioned, a high resistance substrate (*i.e.*, a low austempering temperature) was selected to evaluate the sliding wear behavior of the PVD coated ADI samples.

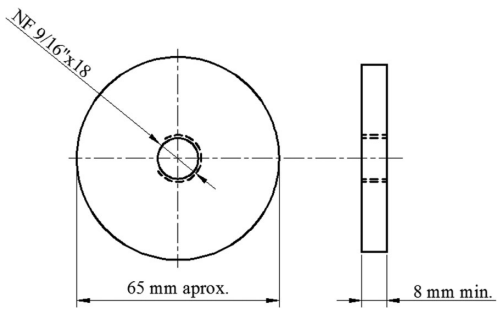

Fig. 1. Scheme of the sliding test samples geometry and dimensions.

2.2. Samples Surface Finishing

The austempered samples were subjected to two different surface finishing methods: manual polishing and grinding. Conventional surface grinding was carried out on a horizontal–spindle (peripheral) surface grinder under industrial–use cutting conditions. Three roughing passes and one finishing pass were conducted on each sample. The finishing pass aims to attain low surface roughness. A vitrified wheel with SiC abrasive grains, identified as IC36/46I/J5V9, was employed. A 5% aqueous solution of soluble oil was used as cooling fluid. Manual polishing was performed using SiC waterproof paper. The final grit size was adjusted to obtain a similar arithmetic average roughness for both surface finishing methods. It was found that a progressive polishing of up to 220 grit size fulfilled this requirement.

2.3. PVD Coating Process

CrN and TiN coatings were applied by arc ion plating (AIP) in an industrial reactor using sets of processing parameters specifically designed for ADI. Prior to this, the samples were thoroughly degreased, ultrasonically cleaned, rinsed with alcohol and dried with warm air. Inside the chamber, and prior to deposition, the samples were cleaned once again by bombardments with energetic ions. **Table 1** lists the process parameters used. The deposition times were adjusted to obtain a similar film thickness for both coating materials.

2.4. Substrates and Coatings Characterization

Average nodule count of the samples was determined by optical microscopy and digital image processing, taking a 5 μm diameter nodule as threshold value. The average nodule count obtained was 497 nod/mm^2. The Brinell hardness (187.5 kg) of the substrates was measured by using an universal hardness tester. The average Brinell hardness obtained was 417 $HBW_{2.5/187.5}$.

Phase identification and residual stress measurements in the uncoated and coated samples were performed by x–ray diffraction (XRD). A Phillips XPERT–PRO diffractometer was utilized, with Cu Kα radiation (λ=1.54187 Å) at 40 kV and 40 mA. XRD patterns for phase identification were

Table 1. Deposition parameters of CrN and TiN coatings.

Coating material	CrN	TiN
Substrate–target distance [mm]	200	200
Substrate BIAS voltage [V]	−175	−175
Arc current [A]	60	60
Chamber pressure [Pa]	2	1.5
Substrate temperature [°C]	300	300
Deposition time [min]	150	180

recorded in a 2θ range from 30° to 90° in steps of 0.02° and with a counting time of 1 second per step. The degree of preferred orientation for the coatings was determined by the calculation of a texture coefficient, *Tc*, defined as:

$$Tc = \frac{I_n(hkl) \big/ I_0(hkl)}{\frac{1}{n}\sum_{1}^{n} I_n(hkl) \big/ I_0(hkl)},$$

where $I_n(hkl)$ is the measured relative intensity of the reflection from the (hkl) plane, $I_0(hkl)$ is the relative intensity from the same plane in a standard reference sample and n is the total number of reflection peaks from the coating. The value of the texture coefficient for the peak under investigation ranges from unity for a randomly oriented sample, to n for a sample having a complete preferential orientation.[26)]

Residual stress measurements were conducted using the $\sin^2\psi$ method, with the assumption of a biaxial stress state. The optimal diffraction peaks for measurements on the coated samples were CrN and TiN (422). The 2θ angle ranged from 125° to 135° for CrN and from 120° to 132° for TiN, with a 2θ step of 0.05° and 5 seconds per step. The peak profiles were recorded at ψ tilt angles of 0°, 25.29°, 37.17°, 47.73° and 58.69°, respectively. The optimal diffraction peak for measurements on the uncoated samples was Fe–α (222). The 2θ angle ranged from 134° to 140°, with a 2θ step of 0.05° and 5 seconds per step. The peak profiles were recorded at ψ tilt angles of 0°, 26.57°, 39.23°, 50.77° and 63.44° respectively. The x–ray elastic constants (XEC's) used to calculate the stresses in the uncoated and coated samples were obtained from bibliographic data.[27–29)]

The conventional arithmetic average roughness (*Ra*) and surface skewness (*Rsk*) of the uncoated and coated samples were analyzed using a stylus profilometer (Taylor Hobson Surtronic 3+) with a 4 mm evaluation length (cut–off, 0.8 mm). In addition, optical microscopy was utilized for the surface characterization of the samples surface. Coatings thickness was measured on fractured cross sections micrographs, obtained by SEM (JEOL JSM–6460LV). Knoop hardness (15 g load) of the uncoated and coated samples was determined using a microhardness tester. Coating adhesion was evaluated by the Rockwell–C adhesion test (150 kg load), using a universal hardness tester.[30)]

2.5. Sliding Wear Tests

Wear tests under dry sliding conditions were carried out with a pin–on–disc tribometer (ASTM G99), using 6 mm AISI 52100 bearing balls as pins. Three tests were carried out for each sample variant, which were conducted in the ambient atmosphere, along a circular track of radius 25 mm, at 0.3 m/s linear speed and 10 N load. The sliding distance was 3 000 m. The friction force was continuously monitored by means of a force transducer. Both the pins and the discs were degreased, cleaned thoroughly in water and dried in acetone prior to the tests. The wear track of the discs was examined by using optical microscopy and stylus profilometry. The pins and discs were weighted before and after the test, using an electronic balance with 0.1 mg resolution. The wear rate was determined by the calculation of a specific wear rate coefficient, K_i, defined as:

$$K_i = \frac{\Delta V_i}{F_N . L},$$

where ΔV_i is the volume loss, F_N is the normal load and L is the sliding distance. Index i identifies the surface considered.[31)]

3. Results and Discussion

3.1. Substrates and Coatings Characteristics

3.1.1. XRD Characterization

Figure 2 illustrates, as an example, typical x–ray spectrums of uncoated and coated ADI samples. The spectrums of the coated samples not only reveal the coatings main diffraction peaks but also some substrates peaks, since the penetration depth of the x–rays is greater than the film thickness.

Figure 3 shows the texture coefficients of the CrN and TiN coatings for the different surface finishing methods analyzed. The reported coefficients correspond to the three most intense peaks. It can be noted that regardless of the surface finishing method employed, CrN and TiN coatings were grown with a preferred orientation of (220) and (111) planes parallel to the surface, respectively.

3.1.2. Surface Topography

Figure 4 shows surface micrographs of the polished and ground samples before coating deposition. In the polished samples, the presence of surface nodules can be noticed while in the ground samples, nodules at the surface cannot be seen. According to a previous study,[32)] this feature is ascribed to the plastic deformation of the metallic matrix, inherent to abrasive cutting of grinding, which covers the nodules.

Figure 5 compares the *Ra* and *Rsk* values of the uncoated and coted samples. As can be noticed, according to what was intended, the *Ra* values of the uncoated samples are similar for both surface finishing methods. However, the polished samples are characterized by the presence of craters on their surface ($Rsk<0$) due to the partial or complete graphite removal of certain surface nodules during the surface finishing stage,[33)] while the ground samples show more symmetric profiles ($Rsk\sim0$) since the surface nodules are covered with a layer of the metal matrix material. On the other hand, the deposition processes alter the surface roughness of the samples, leading to an increase in *Ra* and to a change in *Rsk* due to the attachment of macroparticles to the film during deposition.[34,35)]

3.1.3. Film Thickness, Hardness and Residual Stresses (RS)

Table 2 reports the film thickness, hardness and RS val-

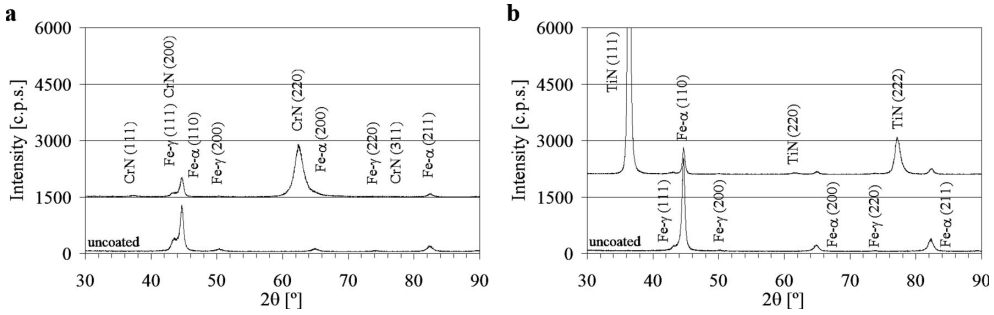

Fig. 2. Diffraction patterns of the uncoated and coated samples: (a) ADI ground–CrN, (b) ADI polished–TiN.

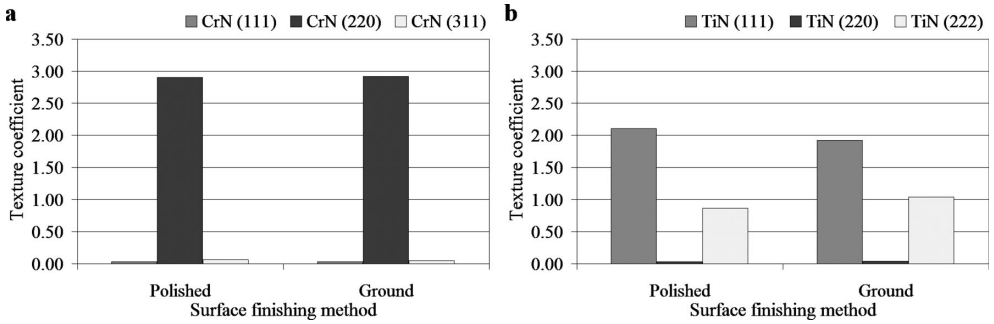

Fig. 3. Texture coefficient of the coatings: (a) ADI–CrN, (b) ADI–TiN.

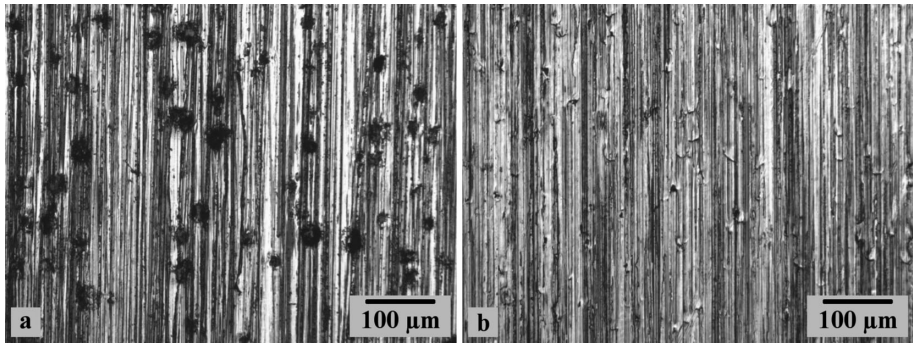

Fig. 4. Samples surface micrographs before coating deposition: (a) ADI polished, (b) ADI ground.

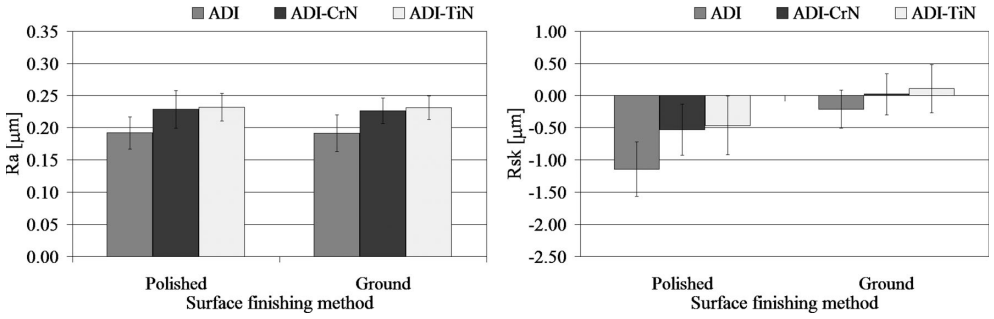

Fig. 5. Roughness parameters of the uncoated and coated samples.

ues of the uncoated and coated samples.

As expected, film thickness is similar for both coatings materials. The Knoop microhardness of the uncoated and coated samples varies with the surface finishing method employed. Ground samples yield higher values due to the surface hardening produced by the abrasive cutting. According to the literature, the values of the CrN coated samples are lower than those of the TiN coated ones. The RS of the uncoated samples are compressive and vary with the surface finishing method employed. The RS values of polished samples are higher than those of ground samples. The RS of coated samples are also compressive and do not vary with the different surface finishing methods employed. The RS values of the CrN coated samples are significantly lower than those of the TiN coated ones. Based on a previous report,[24] the RS of uncoated and coated samples do not

change by varying the measurement direction on the sample surface, thus indicating a rotationally symmetric biaxial stress states.

3.1.4. Adhesion Strength

The adhesion strength quality of CrN and TiN coatings to polished and ground substrates, as determined by the Rockwell–C adhesion test, can be classified as HF1. No delaminations occurred. **Figure 6** illustrates, as an example, the imprints resulting from the Rockwell–C adhesion test.

3.2. Sliding Wear Behavior

Figure 7 shows the friction coefficient evolution for the uncoated and coated samples as a function of the sliding distance, for the different surface finishing methods employed. It can be seen that the behavior of the polished and ground samples is quite similar.

The uncoated samples show an initial friction coefficient close to 0.2, which after the running–in period reaches a steady–state value close to 0.8. Moreover, the polished variant exhibit a running–in period of about 1 000 m while the ground one shows a shorter running–in period (close to 500 m). The longer running–in period of the polished samples with respect to the ground ones relies on the higher exposure of surface graphite nodules, as shown in Fig. 4. On the other hand, the CrN coated samples show an initial friction coefficient close to 0.4, which during the running–in period reaches peaks of about 0.6 and then a steady–state value close to 0.4 again. The running–in period of the polished variant is shorter than that of the ground one (~750 and 1 500 m, respectively). Finally, the TiN coated samples show an initial friction coefficient of about 0.3, which after the running–in period reaches a steady–state value also close to 0.8. In this case, the running–in period of the polished variant is also shorter than that of the ground one (~500 and 1 000 m, respectively).

Table 2. Film thickness, hardness and residual stresses values of the uncoated and coated samples.

Surface finishing	Sample	Film thickness [μm]	Hardness [$HK_{0.015}$]	Residual stresses [GPa]
Polished	ADI	–	375 ± 55	–0.95 ± 0.04
	ADI–CrN	2.46 ± 0.36	1 529 ± 90	–3.34 ± 0.10
	ADI–TiN	2.42 ± 0.60	2 372 ± 104	–5.95 ± 0.14
Ground	ADI	–	723 ± 87	–0.66 ± 0.03
	ADI–CrN	2.38 ± 0.12	1 873 ± 99	–3.27 ± 0.11
	ADI–TiN	2.51 ± 0.52	2 796 ± 121	–5.94 ± 0.13

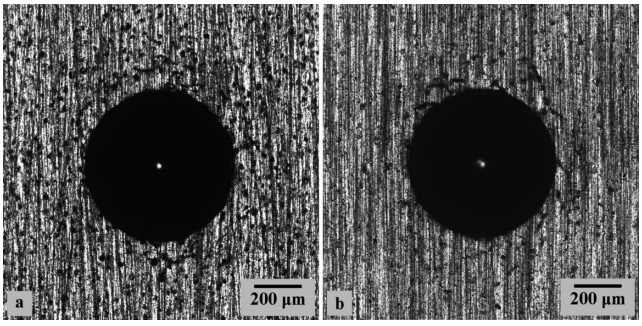

Fig. 6. Imprints on coated samples after Rockwell–C adhesion test: (a) ADI polished–CrN, (b) ADI ground–TiN.

The steady–state values obtained for ADI are very similar to those reported in a previous work,[21] in which 6 mm diameter cemented tungsten carbide (WC) pins and the same testing conditions were employed. On the other hand, the steady–state friction coefficient of the CrN and TiN coated samples are near the lower and upper limits of the ranges reported in the literature, respectively, for CrN and TiN coatings deposited by PVD techniques on aluminum and steel substrates and tested against steel, aluminum, WC, alumina (Al_2O_3) and silicon nitride (Si_3N_4) pins.[36–43]

Figure 8 shows the wear track of the uncoated and coated samples, for the different surface finishing methods analyzed. It can be noted that the sliding wear tests do not produce the fracture and/or delamination of the films in any case. Inside the wear track of the coated samples it can be seen the characteristics scratches of each surface finishing process, indicating negligible wear. Furthermore, in one edge of the ADI ground–TiN wear track (Fig. 8(f)) it can be clearly seen portions of the pin material adhered to the disc surface.

Figures 9 and **10** show the roughness profile of the polished and ground samples, respectively, inside and outside the wear track. It can be seen that the roughness profiles of the coated samples inside and outside the wear track are very similar. Only a slight decrease in the height of the roughness peaks inside the wear track can be appreciated, indicating again negligible wear. On the other hand, the uncoated samples exhibit more significant differences, being possible to observe that inside the wear track the roughness peaks were almost completely swept away, indicting material loss.

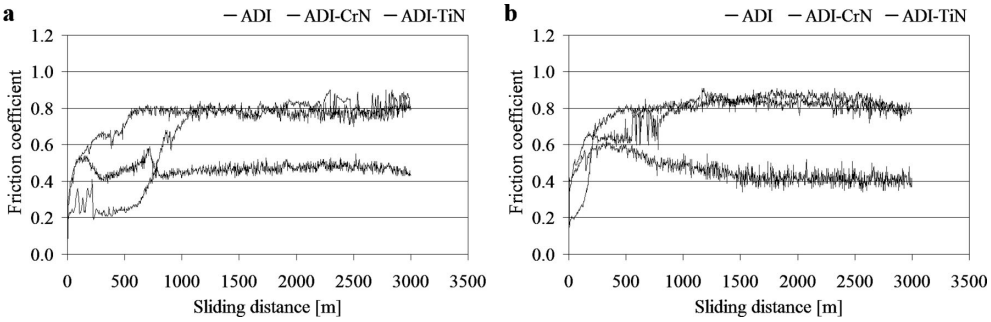

Fig. 7. Friction coefficient evolution of the uncoated and coated samples for the different surface finishing methods employed: (a) polished, (b) ground.

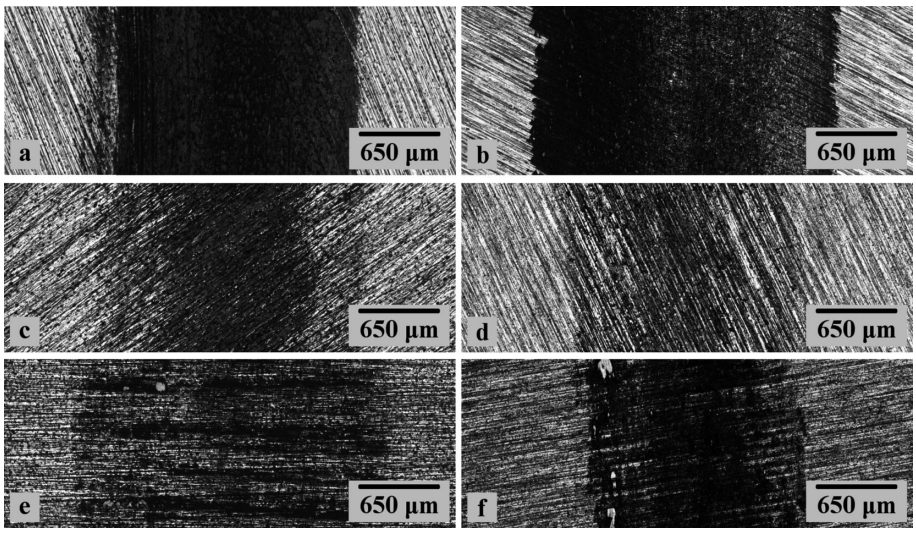

Fig. 8. Wear track of the uncoated and coated samples: (a) ADI polished, (b) ADI ground, (c) ADI polished–CrN, (d) ADI ground–CrN, (e) ADI polished–TiN, (f) ADI ground–TiN.

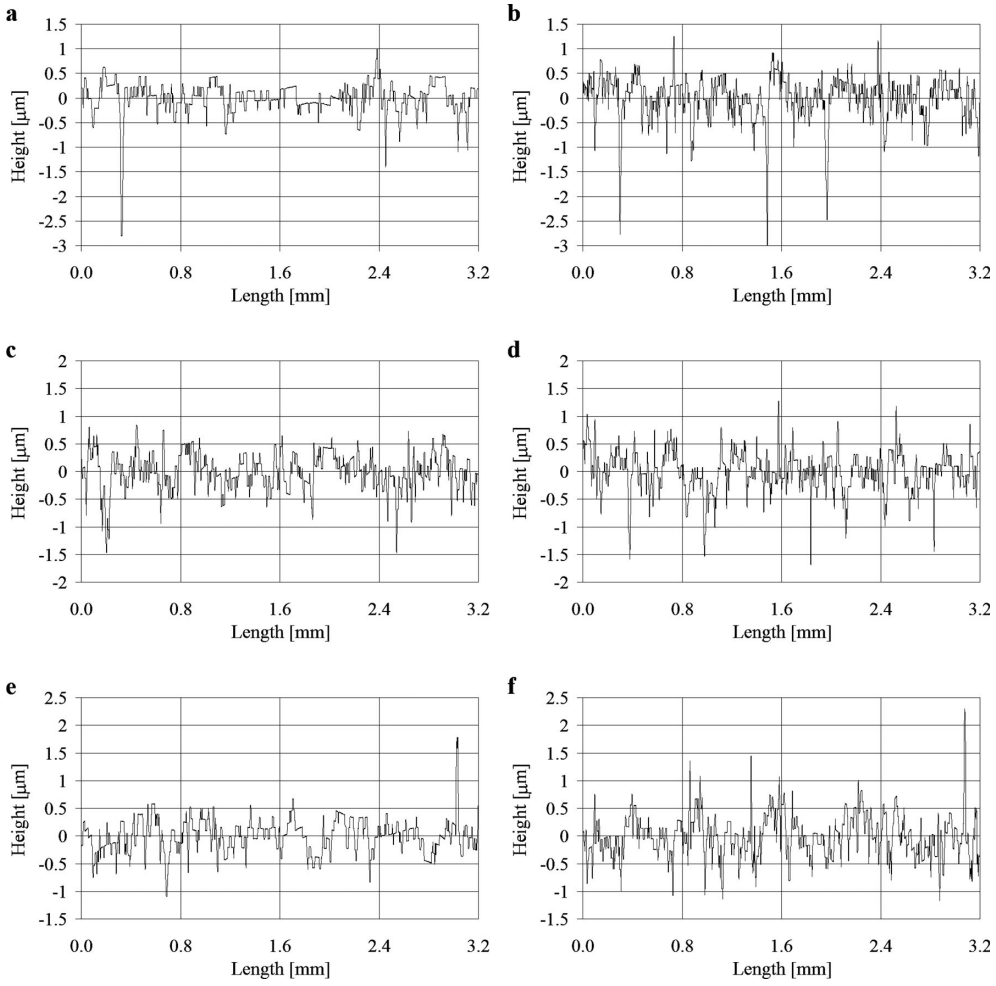

Fig. 9. Roughness profile of the polished samples inside and outside the wear track: (a) ADI inside, (b) ADI outside, (c) ADI–CrN inside, (d) ADI–CrN outside, (e) ADI–TiN inside, (f) ADI–TiN outside.

Figure 11 shows the specific wear rates of the sliding couples in the pin–on–disc test, for the different surface finishing methods employed.

According to what was seen in Figs. 8, 9 and 10, it can be noted that the specific wear rate of the CrN and TiN coated samples is close to zero, while that of the uncoated samples is higher. This behavior is consistent with previous studies performed on PVD TiN, TiA1N, TiCN, and CrN steel coated samples tested against steel and alumina pins.[44,45] The wear rate of the uncoated ground samples is slightly higher than that of the polished ones in spite of their higher hardness. This fact can be ascribed to the lubricating

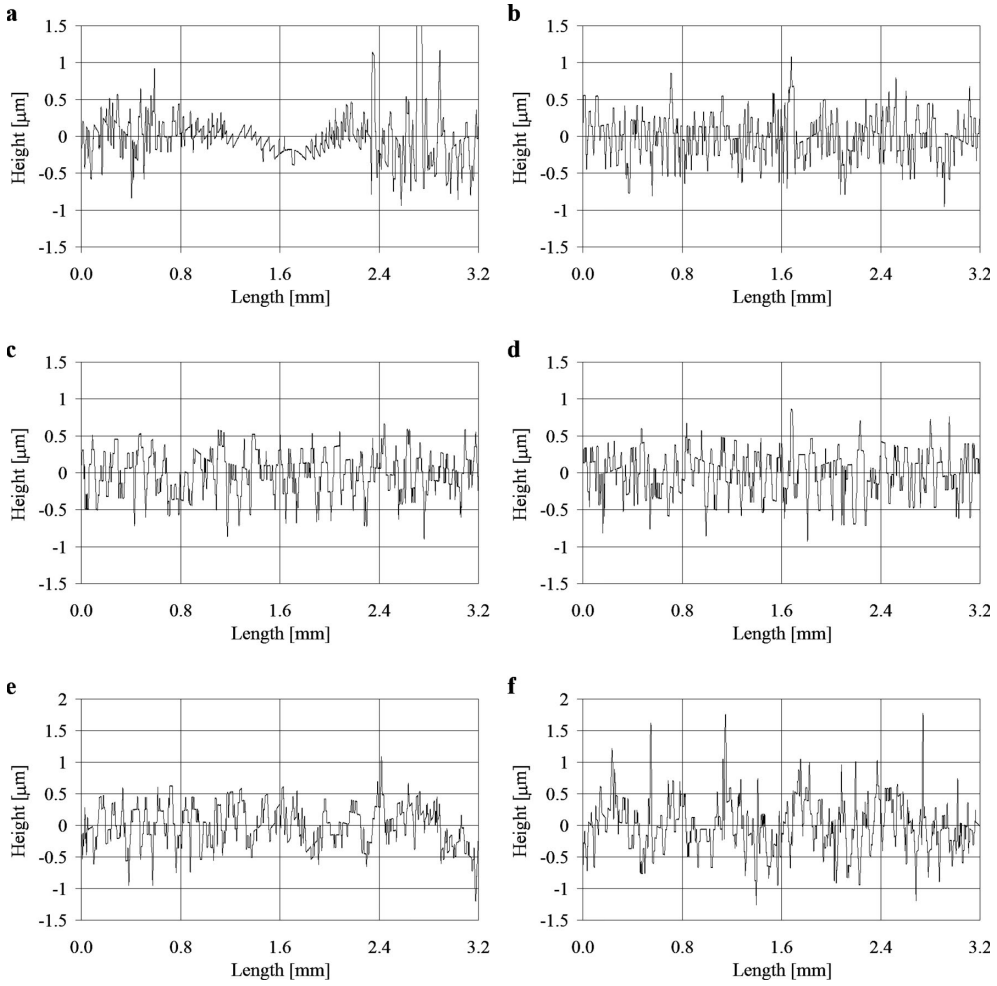

Fig. 10. Roughness profile of the ground samples inside and outside the wear track: (a) ADI inside, (b) ADI outside, (c) ADI–CrN inside, (d) ADI–CrN outside, (e) ADI–TiN inside, (f) ADI–TiN outside.

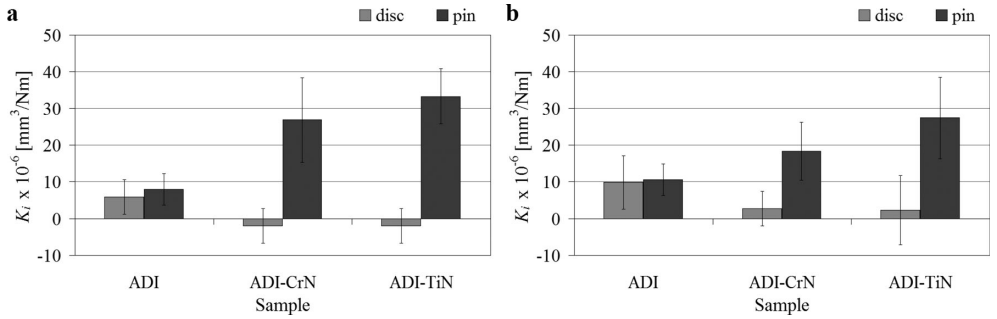

Fig. 11. Specific wear rates of the sliding couples for the different surface finishing methods employed: (a) polished, (b) ground.

effect of the graphite nodules present on the surface of the polished samples. The different characteristics of the coated samples regarding hardness, roughness and RS, obtained by varying the coating material and surface finishing method, do not significantly affect their wear behavior. The negative wear rate of the coated polished samples can be explained by the adhesion of pin material to the disc surface.

On the other hand, the specific wear rate of the pins (AISI 52100 bearing balls) is higher than that of the discs in all the cases, as reported in a previous work.[43] The wear rate of the pins tested against the uncoated ground samples is higher than that of the pins tested against the polished ones. This fact can be explained again by the lubricating effect of the graphite nodules present on the surface of the polished samples and by the higher hardness of the ground samples. The wear rate of the pins tested against the TiN coated samples is higher than that of the pins tested against the CrN coated ones, for the different surface finishing methods employed. This behavior is consistent with a previous report,[43] and can be ascribed to the higher hardness of the TiN coated samples. In addition, some influence of the surface finishing method on the wear rate of the pins tested against the coated samples can be seen. The polished samples, characterized by negative skewness (*i.e.*, a greater con-

tact area), inflict a higher pin wear rate.

4. Conclusions

(1) The uncoated samples show an initial friction coefficient close to 0.2, which after the running–in period reaches a steady–state value close to 0.8. The TiN coated samples show an initial friction coefficient of about 0.3, which after the running–in period also reaches a steady–state value close to 0.8. The CrN coated samples show an initial friction coefficient close to 0.4, which during the running–in period reaches peaks of about 0.6 and then a steady–state value close to 0.4 again.

(2) The sliding wear tests do not produce the fracture and/or delamination of the films in any case. The specific wear rate of the CrN and TiN coated samples is close to zero, while that of the uncoated samples is higher. The wear rate of the uncoated samples is slightly higher fo the ground ones ones due to the lubricating effect of the surface graphite nodules present on the polished samples. The different characteristics of the coated samples regarding hardness, roughness and RS, obtained by varying the coating material and surface finishing method, do not affect their wear behavior.

(3) The specific wear rate of the pins is higher than that of the discs in all the cases. The wear rate of the pins tested against the uncoated samples is higher for the ground ones due to their higher hardness and the lubricating effect of the surface graphite nodules present on the polished samples. The wear rate of the pins tested against the coated samples is higher for the TiN coated ones due to the higher hardness of the TiN coating. The surface finishing method affects the wear rate of the pins tested against the coated samples since polished samples, characterized by negative skewness, inflict a higher pin wear rate.

Acknowledgments

The authors wish to thank the company Sudosilo S.A. for its generous collaboration in coatings deposition. The financial support granted by the CONICET and the National University of Mar del Plata is also gratefully acknowledged.

REFERENCES

1) R. A. Martinez, R. E. Boeri and J. A. Sikora: *Trans. Am. Foundry Soc.*, **106** (1998), 27.
2) J. R. Keough: *Eng. Cast. Solut.*, **3** (2001), 42.
3) P. David, J. Massone, R. Boeri and J. Sikora: *ISIJ Int.*, **44** (2004), 1180.
4) Y. S. Lerner and G. R. Kingsbury: *J. Mater. Eng. Perform.*, **7** (1998), 48.
5) A. R. Ghaderi, M. Nili Ahmadabadi and H. M. Ghasemi: *Wear*, **255** (2003), 410.
6) J. Zimba, M. Samandi, D. Yu, T. Chandra, E. Navara and D. J. Simbi: *Mater. Des.*, **25** (2004), 431.
7) U. Ritha Kumari and P. Prasad Rao: *J. Mater. Sci.*, **44** (2009), 1082.
8) A. S. M. A. Haseeb, M. A. Islam and M. M. A. Bepari: *Wear*, **244** (2000), 15.
9) M. J. Pérez, M. M. Cisneros and H. F. López: *Wear*, **260** (2006), 879.
10) M. Nili Ahmadabadi, H. M. Ghasemi and M. Osia: *Wear*, **231** (1999), 293.
11) G. Straffelini, C. Giuliari, M. Pellizzari, E. Veneri and M. Bronzato: *Wear*, **271** (2011), 1602.
12) A. Roy and I. Manna: *Mater. Sci. Eng. A*, **297** (2001), 85.
13) A. Amirsadeghi and M. Heydarzadeh Sohi: *J. Mater. Process. Technol.*, **201** (2008), 673.
14) A. Amirsadeghi, M. Heydarzadeh Sohi and S. F. Kashani Bozorg: *J. Iron Steel Res. Int.*, **15** (2008), 86.
15) M. Shamanian, S. M. R. Mousavi Abarghouie and S. R. Mousavi Pour: *Mater. Des.*, **31** (2010), 2760.
16) Y. Kayali, Y. Yalçin and Ş. Taktak: *Mater. Des.*, **32** (2011), 4295.
17) H. P. Feng, S. C. Lee, C. H. Hsu and J. M. Ho: *Mater. Chem. Phys.*, **59** (1999), 154.
18) C. H. Hsu, J. K. Lu and R. J. Tsai: *Mater. Sci. Eng. A*, **398** (2005), 282.
19) C. H. Hsu, M. L. Chen and K. L. Lai: *Mater. Sci. Eng. A*, **421** (2006), 182.
20) C. H. Hsu, C. Y. Lee, K. L. Chen and J. H. Lu: *Thin Solid Films*, **517** (2009), 5248.
21) C. H. Hsu, K. L. Chen and K. C. Lu: *Thin Solid Films*, **519** (2011), 4855.
22) D. A. Colombo, M. D. Echeverría, O. J. Moncada and J. M. Massone: *ISIJ Int.*, **51** (2011), 448.
23) D. A. Colombo, M. D. Echeverría, O. J. Moncada and J. M. Massone: *ISIJ Int.*, **52** (2012), 121.
24) D. A. Colombo, M. D. Echeverría, O. J. Moncada and J. M. Massone: *ISIJ Int.*, **53** (2013), 520.
25) D. A. Colombo, M. D. Echeverría, S. Laino, R. C. Dommarco and J. M. Massone: *Wear*, **308** (2013), 35.
26) M. I. Jones, I. R. McColl and D. M. Grant: *Surf. Coat. Technol.*, **132** (2000), 143.
27) K. J. Martinschitz, R. Daniel, C. Mitterer and J. Keckes: *Thin Solid Films*, **516** (2008), 1972.
28) C. J. Smithells and E. A. Brandes: Metals Reference Book, 5th ed, Butterworth, London, (1976), 975.
29) M. Zhang and J. He: *Surf. Coat. Technol.*, **142**–**144** (2001), 125.
30) W. Heinke, A. Leyland, A. Matthews, G. Berg, C. Friedrich and E. Broszeit: *Thin Solid Films*, **270** (1995), 431.
31) J. F. Archard: *J. Appl. Phys.*, **24** (1953), 981.
32) C. Brunetti, M. V. Leite and G. Pintaude: *Wear*, **263** (2007), 663.
33) J. M. Radzikowska: *Mater. Charact.*, **54** (2005), 287.
34) J. M. Cairney, S. G. Harris, L. W. Ma, P. R. Munroe and E. D. Doyle: *J. Mater. Sci.*, **39** (2004), 3569.
35) M. Egawa, K. Miura, M. Yokoi and I. Ishigami: *Surf. Coat. Technol.*, **201** (2007), 4873.
36) S. Y. Yoon, J. K. Kim and K. H. Kim: *Surf. Coat. Technol.*, **161** (2002), 237.
37) P. Harlin, P. Carlsson, U. Bexell and M. Olsson: *Surf. Coat. Technol.*, **201** (2006), 4253.
38) Y. Tanno and A. Azushima: *Wear*, **266** (2009), 1178.
39) E. E. Vera, M. Vite, R. Lewis, E. A. Gallardo and J. R. Laguna-Camacho: *Wear*, **271** (2011), 2116.
40) P. van Essen, R. Hoy, J. D. Kamminga, A. P. Ehiasarian and G. C. A. M. Janssen: *Surf. Coat. Technol.*, **200** (2006), 3496.
41) G. A. Zhang, P. X. Yan, P. Wang, Y. M. Chen and J. Y. Zhang: *Mater. Sci. Eng. A*, **460**–**461** (2007), 301.
42) F. Zhou, K. Chen, M. Wang, X. Xu, H. Meng, M. Yu and Z. Dai: *Wear*, **265** (2008), 1029.
43) Y. H. Cheng, T. Browne and B. Heckerman: *Wear*, **271** (2011), 775.
44) E. J. Bienk, H. Reitz and N. J. Mikkelsen: *Surf. Coat. Technol.*, **76**–**77** (1995), **Part 2**, 475.
45) S. C. Lee, W. Y. Ho and F. D. Lai: *Mater. Chem. Phys.*, **43** (1996), 266.